Evidence of the Purely Leptonic Decay $B^- \to \tau^- \bar{\nu}_\tau$

K. Ikado,[18] K. Abe,[6] K. Abe,[39] I. Adachi,[6] H. Aihara,[41] K. Akai,[6] M. Akemoto,[6] D. Anipko,[1] K. Arinstein,[1] V. Aulchenko,[1] T. Aushev,[9] T. Aziz,[37] A. M. Bakich,[36] V. Balagura,[9] M. Barbero,[5] A. Bay,[14] I. Bedny,[1] K. Belous,[8] U. Bitenc,[10] I. Bizjak,[10] A. Bondar,[1] A. Bozek,[23] M. Bračko,[6,16,10] T. E. Browder,[5] P. Chang,[22] A. Chen,[20] W. T. Chen,[20] Y. Choi,[35] S. Cole,[36] J. Dalseno,[17] M. Danilov,[9] M. Dash,[45] S. Eidelman,[1] D. Epifanov,[1] J. Flanagan,[6] S. Fratina,[10] K. Furukawa,[6] N. Gabyshev,[1] T. Gershon,[6] A. Go,[20] G. Gokhroo,[37] B. Golob,[15,10] A. Gorišek,[10] H. Ha,[12] J. Haba,[6] K. Hara,[6] T. Hara,[28] N. C. Hastings,[41] K. Hayasaka,[18] H. Hayashii,[19] M. Hazumi,[6] L. Hinz,[14] T. Hokuue,[18] Y. Hoshi,[39] S. Hou,[20] W.-S. Hou,[22] N. Iida,[6] T. Iijima,[18] A. Imoto,[19] K. Inami,[18] A. Ishikawa,[41] H. Ishino,[42] R. Itoh,[6] M. Iwasaki,[41] Y. Iwasaki,[6] T. Kamitani,[6] J. H. Kang,[46] S. U. Kataoka,[19] N. Katayama,[6] H. Kawai,[2] T. Kawasaki,[25] H. Kichimi,[6] E. Kikutani,[6] H. J. Kim,[13] H. O. Kim,[35] K. Kinoshita,[3] H. Koiso,[6] S. Korpar,[16,10] P. Križan,[15,10] P. Krokovny,[1] R. Kulasiri,[3] R. Kumar,[29] C. C. Kuo,[20] A. Kuzmin,[1] Y.-J. Kwon,[46] J. S. Lange,[4] G. Leder,[7] J. Lee,[34] T. Lesiak,[23] A. Limosani,[6] S.-W. Lin,[22] D. Liventsev,[9] D. Marlow,[31] T. Matsumoto,[43] A. Matyja,[23] S. McOnie,[36] S. Michizono,[6] T. Mimashi,[6] W. Mitaroff,[7] K. Miyabayashi,[19] H. Miyata,[25] Y. Miyazaki,[18] R. Mizuk,[9] T. Nagamine,[40] I. Nakamura,[6] T. T. Nakamura,[6] E. Nakano,[27] M. Nakao,[6] S. Nishida,[6] O. Nitoh,[44] S. Noguchi,[19] T. Nozaki,[6] S. Ogawa,[38] Y. Ogawa,[6] K. Ohmi,[6] T. Ohshima,[18] N. Ohuchi,[6] K. Oide,[6] T. Okabe,[18] S. Okuno,[11] S. L. Olsen,[5] Y. Onuki,[25] W. Ostrowicz,[23] H. Ozaki,[6] P. Pakhlov,[9] C. W. Park,[35] H. Park,[13] R. Pestotnik,[10] L. E. Piilonen,[45] A. Poluektov,[1] M. Rozanska,[23] Y. Sakai,[6] T. Schietinger,[14] O. Schneider,[14] C. Schwanda,[7] K. Senyo,[18] M. E. Sevior,[17] M. Shapkin,[8] H. Shibuya,[38] T. Shidara,[6] B. Shwartz,[1] V. Sidorov,[1] A. Sokolov,[8] A. Somov,[3] S. Stanič,[26] M. Starič,[10] H. Stoeck,[36] K. Sumisawa,[28] T. Sumiyoshi,[43] S. Suzuki,[32] O. Tajima,[6] F. Takasaki,[6] K. Tamai,[6] N. Tamura,[25] M. Tanaka,[6] M. Tawada,[6] G. N. Taylor,[17] Y. Teramoto,[27] X. C. Tian,[30] K. Trabelsi,[5] T. Tsuboyama,[6] T. Tsukamoto,[6] S. Uehara,[6] T. Uglov,[9] K. Ueno,[22] Y. Unno,[6] S. Uno,[6] Y. Usov,[1] G. Varner,[5] S. Villa,[14] C. C. Wang,[22] C. H. Wang,[21] Y. Watanabe,[42] E. Won,[12] B. D. Yabsley,[36] A. Yamaguchi,[40] Y. Yamashita,[24] M. Yamauchi,[6] M. Yoshida,[6] Y. Yusa,[45] L. M. Zhang,[33] Z. P. Zhang,[33] V. Zhilich,[1] and D. Zürcher[14]

(Belle Collaboration)

[1]*Budker Institute of Nuclear Physics, Novosibirsk*
[2]*Chiba University, Chiba*
[3]*University of Cincinnati, Cincinnati, Ohio 45221*
[4]*University of Frankfurt, Frankfurt*
[5]*University of Hawaii, Honolulu, Hawaii 96822*
[6]*High Energy Accelerator Research Organization (KEK), Tsukuba*
[7]*Institute of High Energy Physics, Vienna*
[8]*Institute of High Energy Physics, Protvino*
[9]*Institute for Theoretical and Experimental Physics, Moscow*
[10]*J. Stefan Institute, Ljubljana*
[11]*Kanagawa University, Yokohama*
[12]*Korea University, Seoul*
[13]*Kyungpook National University, Taegu*
[14]*Swiss Federal Institute of Technology of Lausanne, EPFL, Lausanne*
[15]*University of Ljubljana, Ljubljana*
[16]*University of Maribor, Maribor*
[17]*University of Melbourne, Victoria*
[18]*Nagoya University, Nagoya*
[19]*Nara Women's University, Nara*
[20]*National Central University, Chung-li*
[21]*National United University, Miao Li*
[22]*Department of Physics, National Taiwan University, Taipei*
[23]*H. Niewodniczanski Institute of Nuclear Physics, Krakow*
[24]*Nippon Dental University, Niigata*
[25]*Niigata University, Niigata*
[26]*Nova Gorica Polytechnic, Nova Gorica*
[27]*Osaka City University, Osaka*
[28]*Osaka University, Osaka*
[29]*Panjab University, Chandigarh*

[30]Peking University, Beijing
[31]Princeton University, Princeton, New Jersey 08544
[32]Saga University, Saga
[33]University of Science and Technology of China, Hefei
[34]Seoul National University, Seoul
[35]Sungkyunkwan University, Suwon
[36]University of Sydney, Sydney NSW
[37]Tata Institute of Fundamental Research, Bombay
[38]Toho University, Funabashi
[39]Tohoku Gakuin University, Tagajo
[40]Tohoku University, Sendai
[41]Department of Physics, University of Tokyo, Tokyo
[42]Tokyo Institute of Technology, Tokyo
[43]Tokyo Metropolitan University, Tokyo
[44]Tokyo University of Agriculture and Technology, Tokyo
[45]Virginia Polytechnic Institute and State University, Blacksburg, Virginia 24061
[46]Yonsei University, Seoul

(Received 9 April 2006; revised manuscript received 18 October 2006; published 22 December 2006)

We present the first evidence of the decay $B^- \to \tau^- \bar{\nu}_\tau$, using 414 fb^{-1} of data collected at the $\Upsilon(4S)$ resonance with the Belle detector at the KEKB asymmetric-energy e^+e^- collider. Events are tagged by fully reconstructing one of the B mesons in hadronic modes. We detect the signal with a significance of 3.5 standard deviations including systematics and measure the branching fraction to be $\mathcal{B}(B^- \to \tau^- \bar{\nu}_\tau) = (1.79^{+0.56}_{-0.49}(\text{stat})^{+0.46}_{-0.51}(\text{syst})) \times 10^{-4}$. This implies that $f_B = 0.229^{+0.036}_{-0.031}(\text{stat})^{+0.034}_{-0.037}(\text{syst})$ GeV and is the first direct measurement of this quantity.

DOI: 10.1103/PhysRevLett.97.251802 PACS numbers: 13.20.He, 13.25.Hw

In the standard model (SM), the purely leptonic decay $B^- \to \tau^- \bar{\nu}_\tau$ [1] proceeds via annihilation of b and $\bar{u}$ quarks to a W^- boson (Fig. 1). It provides a direct determination of the product of the B meson decay constant f_B and the magnitude of the Cabibbo-Kobayashi-Maskawa (CKM) matrix element $|V_{ub}|$. The branching fraction is given by

$$\mathcal{B}(B^- \to \tau^- \bar{\nu}_\tau) = \frac{G_F^2 m_B m_\tau^2}{8\pi}\left(1 - \frac{m_\tau^2}{m_B^2}\right)^2 f_B^2 |V_{ub}|^2 \tau_B, \quad (1)$$

where G_F is the Fermi coupling constant, m_B and m_τ are the B and τ masses, respectively, and τ_B is the B^- lifetime [2]. The expected branching fraction is $(1.59 \pm 0.40) \times 10^{-4}$ using $|V_{ub}| = (4.39 \pm 0.33) \times 10^{-3}$, determined by inclusive charmless semileptonic B decay data [3], $\tau_B = 1.643 \pm 0.010$ ps [3], and $f_B = 0.216 \pm 0.022$ GeV obtained from lattice QCD calculations [4]. Physics beyond the SM, such as supersymmetry or two-Higgs doublet models, could modify $\mathcal{B}(B^- \to \tau^- \bar{\nu}_\tau)$ through the introduction of a charged Higgs boson [5]. Purely leptonic B decays have not been observed before. The most stringent upper limit on $B^- \to \tau^- \bar{\nu}_\tau$ comes from the *BABAR* experiment: $\mathcal{B}(B^- \to \tau^- \bar{\nu}_\tau) < 2.6 \times 10^{-4}$ (90% C.L.) [6]. In this Letter, we present the first evidence for $B^- \to \tau^- \bar{\nu}_\tau$ from the Belle experiment.

We use a 414 fb^{-1} data sample containing 449×10^6 B meson pairs collected with the Belle detector at the KEKB asymmetric-energy e^+e^- (3.5 on 8 GeV) collider [7] operating at the $\Upsilon(4S)$ resonance ($\sqrt{s} = 10.58$ GeV). The Belle detector [8] is a large-solid-angle magnetic spectrometer consisting of a silicon vertex detector, a 50-layer central drift chamber, a system of aerogel threshold Cherenkov counters, time-of-flight scintillation counters, and an electromagnetic calorimeter (ECL) comprised of CsI(Tl) crystals located inside a superconducting solenoid coil that provides a 1.5 T magnetic field. An iron flux return located outside of the coil is instrumented to identify K_L^0 and muons (KLM).

We use a detailed Monte Carlo (MC) simulation based on GEANT [9] to determine the signal selection efficiency and study the background. In order to reproduce the effects of a beam background, data taken with random triggers for each run period are overlaid on simulated events. The $B^- \to \tau^- \bar{\nu}_\tau$ signal decay is generated by the EVTGEN package [10]. To model the background from $e^+e^- \to B\bar{B}$ and continuum $q\bar{q}$ ($q = u, d, s, c$) production processes, large $B\bar{B}$ and $q\bar{q}$ MC samples corresponding to about twice the data sample are used. We also use MC samples for rare B decay processes, such as charmless

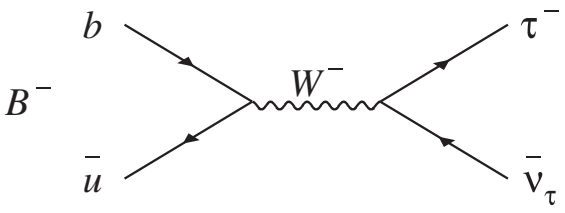

FIG. 1. Purely leptonic B decay proceeds via quark annihilation into a W boson.

hadronic, radiative, electroweak decays and $b \to u$ semileptonic decays.

We fully reconstruct one of the B mesons in the event, referred to hereafter as the tag side ($B_{\rm tag}$), and compare properties of the remaining particle(s), referred to as the signal side ($B_{\rm sig}$), to those expected for signal and background. The method allows us to suppress strongly the combinatorial background from both $B\bar{B}$ and continuum events. In order to avoid experimental bias, the signal region in the data is not examined until the event selection criteria are finalized.

The $B_{\rm tag}$ candidates are reconstructed in the following decay modes: $B^+ \to \bar{D}^{(*)0}\pi^+$, $\bar{D}^{(*)0}\rho^+$, $\bar{D}^{(*)0}a_1^+$, and $\bar{D}^{(*)0}D_s^{(*)+}$. The $\bar{D}^0$ mesons are reconstructed as $\bar{D}^0 \to K^+\pi^-$, $K^+\pi^-\pi^0$, $K^+\pi^-\pi^+\pi^-$, $K_S^0\pi^0$, $K_S^0\pi^-\pi^+$, $K_S^0\pi^-\pi^+\pi^0$, and K^-K^+, and the D_s^+ mesons are reconstructed as $D_s^+ \to K_S^0K^+$ and $K^+K^-\pi^+$. The $\bar{D}^{*0}$ and D_s^{*+} mesons are reconstructed in $\bar{D}^{*0} \to \bar{D}^0\pi^0$, $\bar{D}^0\gamma$, and $D_s^{*+} \to D_s^+\gamma$ modes. The selection of $B_{\rm tag}$ candidates is based on the beam-constrained mass $M_{\rm bc} \equiv \sqrt{E_{\rm beam}^2 - p_B^2}$ and the energy difference $\Delta E \equiv E_B - E_{\rm beam}$. Here E_B and p_B are the reconstructed energy and momentum of the $B_{\rm tag}$ candidate in the e^+e^- center-of-mass (c.m.) system, respectively, and $E_{\rm beam}$ is the beam energy in the c.m. frame. The selection criteria for $B_{\rm tag}$ are defined as $M_{\rm bc} > 5.27$ GeV/c^2 and -80 MeV $< \Delta E < 60$ MeV. If an event has multiple $B_{\rm tag}$ candidates, we choose the one having the smallest χ^2 based on deviations from the nominal values of ΔE, the D candidate mass, and the $D^* - D$ mass difference if applicable. By fitting the $M_{\rm bc}$ distribution to the sum of an empirical parametrization of the background shape [11] plus a signal shape [12], we estimate the number of $B_{\rm tag}$'s and their purity in the selected region to be 6.80×10^5 and 0.55, respectively.

In the events where a $B_{\rm tag}$ is reconstructed, we search for decays of $B_{\rm sig}$ into a τ and a neutrino. Candidate events are required to have one or three charged track(s) on the signal side with the total charge being opposite to that of $B_{\rm tag}$. The τ lepton is identified in the five decay modes $\mu^-\bar{\nu}_\mu\nu_\tau$, $e^-\bar{\nu}_e\nu_\tau$, $\pi^-\nu_\tau$, $\pi^-\pi^0\nu_\tau$, and $\pi^-\pi^+\pi^-\nu_\tau$, which taken together correspond to 81% of all τ decays [2]. The muon, electron, and charged pion candidates are selected based on information from particle identification subsystems. The leptons are selected with efficiency greater than 90% for both muons and electrons in the c.m. momentum region above 1.2 GeV/c and misidentification rates of less than 0.2% (1.5%) for electrons (muons). Kaon candidates are rejected for all charged tracks on the signal side. The π^0 candidates are reconstructed by requiring the invariant mass of two γ's to satisfy $|M_{\gamma\gamma} - m_{\pi^0}| < 20$ MeV/c^2. For all modes except $\tau^- \to \pi^-\pi^0\nu_\tau$, we reject events with π^0 mesons on the signal side. We place the following requirements on the track momentum in the c.m. frame: $p_\ell > 0.3$ GeV/c for $\mu^-\bar{\nu}_\mu\nu_\tau$ and $e^-\bar{\nu}_e\nu_\tau$, $p_{\pi^-} > 1.0$ GeV/c for $\pi^-\nu_\tau$, $p_{\pi^-\pi^0} > 1.2$ GeV/c for $\pi^-\pi^0\nu_\tau$, and $p_{\pi^-\pi^+\pi^-} > 1.8$ GeV/c for $\pi^-\pi^+\pi^-\nu_\tau$. We calculate the missing momentum of the event in the c.m. frame ($p_{\rm miss}$) from p_B and the momenta of charged tracks and π^0's on the signal side. We require $p_{\rm miss} > 0.2$ GeV/c for $\mu^-\bar{\nu}_\mu\nu_\tau$ and $e^-\bar{\nu}_e\nu_\tau$, $p_{\rm miss} > 1.0$ GeV/c for $\pi^-\nu_\tau$, $p_{\rm miss} > 1.2$ GeV/c for $\pi^-\pi^0\nu_\tau$, and $p_{\rm miss} > 1.8$ GeV/c for $\pi^-\pi^+\pi^-\nu_\tau$. In order to suppress background where particles produced along the beam pipe escape detection, the cosine of the angle of the missing momentum ($\cos\theta_{\rm miss}^*$) is required to satisfy $-0.86 < \cos\theta_{\rm miss}^* < 0.95$ in the c.m. frame. We further require the invariant mass of the visible decay products to satisfy $|M_{\pi\pi} - m_\rho| < 0.15$ GeV/c^2 and $|M_{\pi\pi\pi} - m_{a_1^-}| < 0.3$ GeV/c^2. All of the selection criteria have been optimized to achieve the highest sensitivity in MC simulations.

The most powerful variable for separating signal and background is the remaining energy in the ECL, denoted as $E_{\rm ECL}$, which is the sum of the energies of neutral clusters that are not associated with either the $B_{\rm tag}$ or the π^0 candidate from the $\tau^- \to \pi^-\pi^0\nu_\tau$ decay. For neutral clusters contributing to $E_{\rm ECL}$, we require a minimum energy threshold of 50 MeV for the barrel and 100 (150) MeV for the forward (backward) end-cap ECL. A higher threshold is used for the end-cap ECL because the effect of beam background is more severe. For signal events, $E_{\rm ECL}$ must be either zero or a small value arising from beam background hits; therefore, signal events peak at low $E_{\rm ECL}$. On the other hand, background events are distributed toward higher $E_{\rm ECL}$ due to the contribution from additional neutral clusters.

The $E_{\rm ECL}$ signal region is optimized for each τ decay mode based on the MC simulation and is defined by $E_{\rm ECL} < 0.2$ GeV for the $\mu^-\bar{\nu}_\mu\nu_\tau$, $e^-\bar{\nu}_e\nu_\tau$, and $\pi^-\nu_\tau$ modes and $E_{\rm ECL} < 0.3$ GeV for the $\pi^-\pi^0\nu_\tau$ and $\pi^-\pi^+\pi^-\nu_\tau$ modes. The $E_{\rm ECL}$ sideband region is defined by 0.4 GeV $< E_{\rm ECL} < 1.2$ GeV for the $\mu^-\bar{\nu}_\mu\nu_\tau$, $e^-\bar{\nu}_e\nu_\tau$, and $\pi^-\nu_\tau$ modes and by 0.45 GeV $< E_{\rm ECL} < 1.2$ GeV for the $\pi^-\pi^0\nu_\tau$ and $\pi^-\pi^+\pi^-\nu_\tau$ modes. Table I shows the number of events found in the sideband region for data ($N_{\rm side}^{\rm obs}$) and for the background MC simulation ($N_{\rm side}^{\rm MC}$) scaled to the equivalent integrated luminosity in the data. Their good agreement for each τ decay mode indicates the validity of the background MC simulation. According to the MC simulation, about 95% (5%) of the background events come from $B\bar{B}$ ($q\bar{q}$) processes. Table I also shows the number of the background MC events in the signal region ($N_{\rm sig}^{\rm MC}$). The MC simulation predicts that the background in the signal region comes from $B^- \to D^{(*)0}\ell^-\bar{\nu}$ semileptonic decays (90%) and rare B decay processes (10%). About 30% of the background has K_L^0 candidates in the KLM.

In order to validate the $E_{\rm ECL}$ simulation, we use a control sample of double tagged events, where the $B_{\rm tag}$ is fully

TABLE I. The number of observed events in the data in the sideband region ($N_{\rm side}^{\rm obs}$), number of background MC events in the sideband region ($N_{\rm side}^{\rm MC}$) and the signal region ($N_{\rm sig}^{\rm MC}$), number of observed events in data in the signal region ($N_{\rm obs}$), number of signal (N_s) and background (N_b) in the signal region determined by the fit, signal selection efficiencies ($\varepsilon^{\rm sel}$), and the extracted branching fraction ($\mathcal{B}$) for $B^- \to \tau^- \bar{\nu}_\tau$. The listed errors are statistical only. The last column gives the significance of the signal including the systematic uncertainty in the signal yield (Σ).

	$N_{\rm side}^{\rm obs}$	$N_{\rm side}^{\rm MC}$	$N_{\rm sig}^{\rm MC}$	$N_{\rm obs}$	N_s	N_b	$\varepsilon^{\rm sel}(\%)$	$\mathcal{B}(10^{-4})$	Σ
$\mu^-\bar{\nu}_\mu\nu_\tau$	96	94.2 ± 8.0	9.4 ± 2.6	13	$5.6^{+3.1}_{-2.8}$	$8.8^{+1.1}_{-1.1}$	3.64 ± 0.02	$2.57^{+1.38}_{-1.27}$	2.2σ
$e^-\bar{\nu}_e\nu_\tau$	93	89.6 ± 8.0	8.6 ± 2.3	12	$4.1^{+3.3}_{-2.6}$	$9.0^{+1.1}_{-1.1}$	4.57 ± 0.03	$1.50^{+1.20}_{-0.95}$	1.4σ
$\pi^-\nu_\tau$	43	41.3 ± 6.2	4.7 ± 1.7	9	$3.8^{+2.7}_{-2.1}$	$3.9^{+0.8}_{-0.8}$	4.87 ± 0.03	$1.30^{+0.89}_{-0.70}$	2.0σ
$\pi^-\pi^0\nu_\tau$	21	23.3 ± 4.7	5.9 ± 1.9	11	$5.4^{+3.9}_{-3.3}$	$5.4^{+1.6}_{-1.6}$	1.97 ± 0.02	$4.54^{+3.26}_{-2.74}$	1.5σ
$\pi^-\pi^+\pi^-\nu_\tau$	21	18.5 ± 4.1	4.2 ± 1.6	9	$3.0^{+3.5}_{-2.5}$	$4.8^{+1.4}_{-1.4}$	0.77 ± 0.02	$6.42^{+7.58}_{-5.42}$	1.0σ

reconstructed as described above and $B_{\rm sig}$ is reconstructed in the decay chain $B^- \to D^{*0}\ell^-\bar{\nu}$ ($D^{*0} \to D^0\pi^0$), followed by $D^0 \to K^-\pi^+$ or $K^-\pi^-\pi^+\pi^+$, where ℓ is a muon or electron. The sources affecting the $E_{\rm ECL}$ distribution in the control sample are similar to those in the signal MC simulation. Figure 2 shows the $E_{\rm ECL}$ distribution in the control sample for the data and the scaled MC simulation. Their agreement demonstrates the validity of the $E_{\rm ECL}$ simulation in the signal MC simulation.

After finalizing the signal selection criteria, the signal region is examined. Figure 3 shows the $E_{\rm ECL}$ distribution obtained when all τ decay modes are combined. One can see a significant excess of events in the $E_{\rm ECL}$ signal region below $E_{\rm ECL} < 0.25$ GeV. Table I shows the number of events observed in the signal region ($N_{\rm obs}$) for each τ decay mode. For the events in the signal region, we verify that the distributions of the event selection variables other than $E_{\rm ECL}$, such as $M_{\rm bc}$ and $p_{\rm miss}$, are consistent with the sum of the signal and background distributions expected from MC simulations. The excess remains after applying a K_L^0 veto requirement.

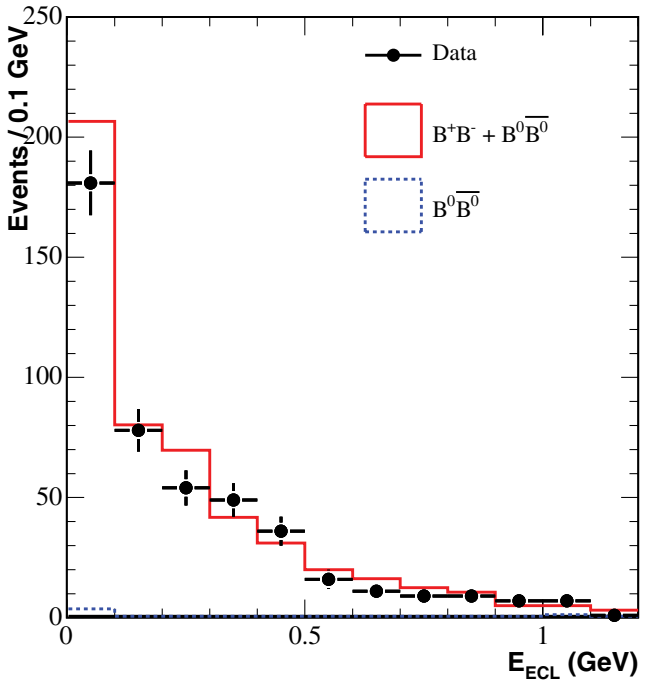

FIG. 2 (color online). $E_{\rm ECL}$ distribution for double tagged events, where one B is fully reconstructed in the hadronic mode and the other B is reconstructed as $B^- \to D^{*0}\ell^-\bar{\nu}$. The dots indicate the data. The solid histogram is the background from $B\bar{B}$ MC events ($B^+B^- + B^0\bar{B}^0$), while the dashed one shows the contribution from $B^0\bar{B}^0$ events.

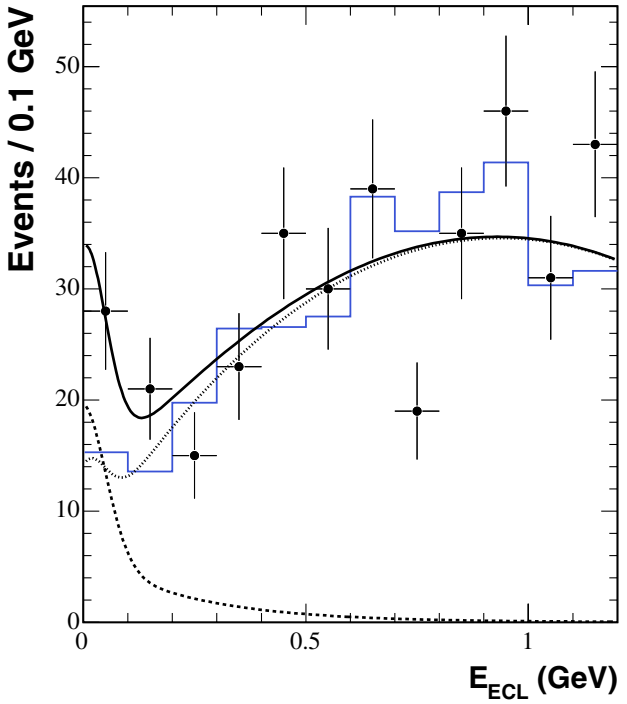

FIG. 3 (color online). $E_{\rm ECL}$ distributions in the data after all selection criteria except the one on $E_{\rm ECL}$. The data and background MC samples are represented by the points and the solid histogram, respectively. The solid curve shows the result of the fit with the sum of the signal (dashed curve) and background (dotted curve) contributions.

We obtain the final results by fitting the obtained $E_{\rm ECL}$ distributions to the sum of the expected signal and background shapes. Probability density functions (PDFs) for the signal $f_s(E_{\rm ECL})$ and for the background $f_b(E_{\rm ECL})$ are constructed for each τ decay mode from the MC simulation. The signal PDF is modeled as the sum of a Gaussian function, centered at $E_{\rm ECL} = 0$, and an exponential function. The background PDF, as determined from the MC simulation, is parametrized by the sum of a Gaussian function and a second-order polynomial function. The Gaussian function in the background PDF addresses deviations from the second-order parametrization, which may arise from a peaking component in the lower $E_{\rm ECL}$. The PDFs are combined into an extended likelihood function

$$\mathcal{L} = \frac{e^{-(n_s+n_b)}}{N!}\prod_{i=1}^{N}(n_s f_s(E_i) + n_b f_b(E_i)), \qquad (2)$$

where E_i is the $E_{\rm ECL}$ in the ith event, N is the total number of events in the data, and n_s and n_b are the signal yield and background yield, respectively, to be determined by the fit to the whole $E_{\rm ECL}$ region ($0 < E_{\rm ECL} < 1.2$). The results are listed in Table I. Table I also gives the number of background events in the signal region deduced from the fit (N_b), which is consistent with the expectation from the background MC simulation ($N_{\rm sig}^{\rm MC}$).

The branching fractions are calculated as $\mathcal{B} = N_s/(2\varepsilon N_{B^+B^-})$, where $N_{B^+B^-}$ is the number of $\Upsilon(4S) \to B^+B^-$ events, assuming $N_{B^+B^-} = N_{B^0\bar{B}^0}$. The efficiency is defined as $\varepsilon = \varepsilon^{\rm tag} \times \varepsilon^{\rm sel}$, where $\varepsilon^{\rm tag}$ is the tag reconstruction efficiency for events with $B^- \to \tau^-\bar{\nu}_\tau$ decays on the signal side, determined by MC simulations to be 0.136 ± 0.001(stat)%, and $\varepsilon^{\rm sel}$ is the event selection efficiency listed in Table I, as determined by the ratio of the number of events surviving all of the selection criteria including the τ decay branching fractions to the number of fully reconstructed $B^\pm$. The branching fraction for each τ decay mode is consistent within errors. To obtain the combined result for all τ decay modes, we multiply the likelihood functions to produce the combined likelihood ($\mathcal{L}_{\rm com} = \prod_{j=1}^{5}\mathcal{L}_j$) and constrain the five signal components by a single branching fraction. The combined fit gives $17.2^{+5.3}_{-4.7}$ signal events in the signal region (N_s) and $24.1^{+7.6}_{-6.6}$ in the entire region (n_s). The branching fraction is found to be $(1.79^{+0.56}_{-0.49}) \times 10^{-4}$.

Systematic errors for the measured branching fraction are associated with the uncertainties in the number of B^+B^-, signal yields, and efficiencies. The systematic error due to the uncertainty in $N_{B^+B^-}$ is 1%. The uncertainty in the signal yields arises from uncertainties in the signal and background shape and is determined to be $^{+23\%}_{-26\%}$. Here the uncertainty due to the signal shape uncertainty is determined by varying the signal PDF parameters by the amount of difference of each parameter between the data and MC simulations for the control sample of double tagged events. To determine the background shape uncertainty, we vary the Gaussian constant of the background PDF by the branching fraction errors from [2] for the dominant peaking background sources [such as $B \to D^{(*)0}\ell\nu$, $D^0 \to \pi(K)\ell\nu$, etc.]. We then add in quadrature the variations for the signal and background shapes. We take a 10.5% error as the systematic error associated with the tag reconstruction efficiency from the difference of yields between the data and MC simulations for the control sample. This value includes the error in the branching fraction $\mathcal{B}(B^- \to D^{*0}\ell^-\bar{\nu})$, which we estimate from $\mathcal{B}(B^0 \to D^{*-}\ell^+\nu)$ in Ref. [2] and isospin symmetry. The systematic error in the signal efficiencies depends on the τ decay mode and arises from the uncertainty in tracking efficiency (1%–3%), π^0 reconstruction efficiency (3%), particle identification efficiency (2%–6%), branching fractions of τ decays (0.3%–1.1%), and MC statistics (0.6%–2%). These efficiency errors sum up to 5.6% for the combined result after taking into account the correlations between the five τ decay modes [13]. The total fractional systematic uncertainty of the combined measurement is $^{+26\%}_{-28\%}$, and the branching fraction is

$$\mathcal{B}(B^- \to \tau^-\bar{\nu}_\tau) = (1.79^{+0.56}_{-0.49}(\text{stat})^{+0.46}_{-0.51}(\text{syst})) \times 10^{-4}.$$

The significance is 3.5σ when all τ decay modes are combined, where the significance is defined as $\Sigma = \sqrt{-2\ln(\mathcal{L}_0/\mathcal{L}_{\rm max})}$, where $\mathcal{L}_{\rm max}$ and $\mathcal{L}_0$ denote the maximum likelihood value and likelihood value obtained assuming zero signal events, respectively. Here the likelihood function from the fit is convolved with a Gaussian systematic error function in order to include the systematic uncertainty in the signal yield.

In conclusion, we have found the first evidence of the purely leptonic decay $B^- \to \tau^-\bar{\nu}_\tau$ from a data sample of 449×10^6 $B\bar{B}$ pairs collected at the $\Upsilon(4S)$ resonance with the Belle experiment. The signal has a significance of 3.5 standard deviations. The measured branching fraction is $(1.79^{+0.56}_{-0.49}(\text{stat})^{+0.46}_{-0.51}(\text{syst})) \times 10^{-4}$. The result is consistent with the SM prediction within errors. Using the measured branching fraction and known values of G_F, m_B, m_τ [2], and τ_B [3], the product of the B meson decay constant f_B and the magnitude of the CKM matrix element $|V_{ub}|$ is determined to be $f_B|V_{ub}| = (10.1^{+1.6}_{-1.4}(\text{stat})^{+1.3}_{-1.4}(\text{syst})) \times 10^{-4}$ GeV. Using the value of $|V_{ub}|$ from Ref. [3], we obtain $f_B = 0.229^{+0.036}_{-0.031}(\text{stat})^{+0.034}_{-0.037}(\text{syst})$ GeV, the first direct determination of the B meson decay constant.

We thank the KEKB group for excellent operation of the accelerator, the KEK cryogenics group for efficient solenoid operations, and the KEK computer group and the NII for valuable computing and Super-SINET network support. We acknowledge support from MEXT and JSPS (Japan); ARC and DEST (Australia); NSFC and KIP of CAS (Contracts No. 10575109 and No. IHEP-U-503, China); DST (India); the BK21 program of MOEHRD,

and the CHEP SRC and BR (Grant No. R01-2005-000-10089-0) programs of KOSEF (Korea); KBN (Contract No. 2P03B 01324, Poland); MIST (Russia); ARRS (Slovenia); SNSF (Switzerland); NSC and MOE (Taiwan); and DOE (USA).

[1] Charge conjugate states are implied throughout the Letter.

[2] S. Eidelman *et al.* (Particle Data Group), Phys. Lett. B **592**, 1 (2004).

[3] E. Barberio *et al.* (Heavy Flavor Averaging Group), hep-ex/0603003.

[4] A. Gray *et al.* (HPQCD Collaboration), Phys. Rev. Lett. **95**, 212001 (2005); see also S. Hashimoto, Int. J. Mod. Phys. A **20**, 5133 (2005), which quotes an average value of 0.189 ± 0.027 GeV. QCD sum rules predict $f_B = 210 \pm 19$ MeV; see M. Jamin and B. O. Lange, Phys. Rev. D **65**, 056005 (2002).

[5] W. S. Hou, Phys. Rev. D **48**, 2342 (1993).

[6] B. Aubert *et al.* (*BABAR* Collaboration), Phys. Rev. D **73**, 057101 (2006).

[7] S. Kurokawa and E. Kikutani, Nucl. Instrum. Methods Phys. Res., Sect. A **499**, 1 (2003).

[8] A. Abashian *et al.* (Belle Collaboration), Nucl. Instrum. Methods Phys. Res., Sect. A **479**, 117 (2002).

[9] R. Brun *et al.*, GEANT3.21, CERN Report No. DD/EE/84-1, 1984.

[10] See the EVTGEN package home page, http://www.slac.stanford.edu/~lange/EvtGen/.

[11] H. Albrecht *et al.* (ARGUS Collaboration), Phys. Lett. B **185**, 218 (1987).

[12] E. D. Bloom and C. Peck, Annu. Rev. Nucl. Part. Sci. **33**, 143 (1983).

[13] L. Lyons, D. Gibaut, and P. Clifford, Nucl. Instrum. Methods Phys. Res., Sect. A **270**, 110 (1988).